

# In Silico Screening and Evolution of Promising Novel Anti-Virulents Against Salmonella ATPase

Lexi Xu<sup>1</sup> and Norah Shen<sup>#</sup>

<sup>1</sup>Leland High School, USA

<sup>#</sup>Advisor

## ABSTRACT

Current treatments for bacterial infections are under threat by the growth of antibiotic resistance in many different pathogens. Of these pathogens, *Salmonella* is a particularly widespread microbe, infecting over a million people annually as the leading source of food-borne diseases. One potential solution for antibiotic-resistant *Salmonella* is virulence inhibition of the bacteria's T3SS injection system, which has been shown to destroy *Salmonella*'s proliferative abilities. Here, we identify fourteen compounds, primarily novel ligands, that exhibit high in-vitro potential as *Salmonella* inhibitors by attacking the ATPase InvC protein vital for T3SS injection—an enzyme that has not been previously evaluated for small-molecule inhibition. We also present a statistical analysis of AutoGrow4, a virtual structure-based molecular design tool that evolves ligands to better suit a target protein using Autodock Vina binding affinity calculations. Together, these create an entirely open-source workflow towards computational identification and evaluation of novel chemical treatments.

## Introduction

Antibiotic resistance has become one of the leading threats to human health worldwide in the face of widespread antibiotic abuse and lack of new pharmaceutical treatments<sup>1</sup>, with the Global Antimicrobial Resistance and Use Surveillance System (GLASS) report finding that over 50% of bacteria in bloodstream infections are resistant to antibiotics<sup>2</sup>. *Salmonella*, a foodborne pathogen associated with 1.2 million illnesses annually<sup>3</sup>, is particularly dangerous because it has developed resistance to several common antibiotics, including ampicillin, chloramphenicol, streptomycin, antimicrobial sulfonamides, and tetracycline<sup>3</sup>. The CDC estimates that drug-resistant salmonellosis (*Salmonella enterica* & *Salmonella Typhimurium*) accounts for approximately 212,500 infections yearly, and drug-resistant typhoid fever (*Salmonella Typhi* and *Salmonella Paratyphi A.*, two serovars of *Salmonella enterica*) leads to an additional 77,000 infections<sup>4</sup>. Conservative estimates reveal that drug-resistant *Salmonella* causes nearly 300,000 infections annually. The severe threat that *Salmonella* poses urgently calls for the discovery of new drugs or treatment methods effective against drug-resistant *Salmonella*.

One solution to this developing resistance problem is utilizing virulence inhibitors, which convert pathogenic organisms to benign ones by disarming them of their virulence. Many virulence inhibitors target external molecules or effectors, which can evade the development of antibacterial resistance caused by diminished permeability (where antibiotics become impermeable to the bacterial membrane as bacteria close protein channels)<sup>5</sup>. In addition, it has been theorized that even when bacteria develop resistance to anti-virulents, it often results in nonfunctional virulent systems<sup>5</sup>. Another benefit to virulence inhibitors is the relative lack of impact on the patient's microbiome: while traditional antibiotics often target both pathogenic and helpful bacteria, disarming the secretion system virtually exclusive to harmful gram-negative bacteria keeps intestinal flora intact and likely reduces gastrointestinal side effects<sup>6</sup>.

*Salmonella*, like many other gram-negative bacteria (*Bordetella* spp., *Burkholderia* spp., *Chlamydia* spp., *Escherichia coli*, *Pseudomonas aeruginosa*, *Shigella* spp., *Vibrio cholerae*, and *Yersinia* spp), utilizes the

Type 3 Secretion System (T3SS) to secrete its bacterial effectors into the eukaryotic cell<sup>7</sup>. The T3SS is a protein complex comprising over 20 different conserved proteins, creating a channel from the bacterial cell to the host cell<sup>8</sup>, allowing it to “inject” bacteria effectors using a needle-like apparatus known as an injectosome<sup>9</sup>. The T3SS contains 3 types of proteins: structural proteins, which form the body of the apparatus; translocators, which translocate the virulence factors into the host cells; and the effectors, which promote bacterial invasion and survival in the host cell<sup>10</sup>. Its two continuous rings pass through the bacterial inner membrane, outer membrane, and peptidoglycan layer, anchoring the needle to the cell membrane. The structural apparatus contains the cytoplasmic complex, the export apparatus, the basal body, and the 2.5 nm needle<sup>10</sup>(Figure 1). To secrete the effectors, chaperone proteins form complexes with substrates, which are loaded onto free cytoplasmic complexes. SctK, SctQ, and SctL, specifically, are known as the “sorting platform” because of their involvement in recruiting chaperone-substrate complexes<sup>11</sup>. The sorting platform then “unfolds” the effectors to “de-chaperone” them, and the ATPase in the cytoplasmic complex works with the export apparatus to guide and power the secretion of effector proteins through the needle<sup>8</sup>. Effectors are passed through the translocon, which forms pores on the host cell membrane through the needle tip<sup>10</sup>. This signals increased bacterial invasion and promotes bacterial survival, thus killing the host cell<sup>8</sup>.

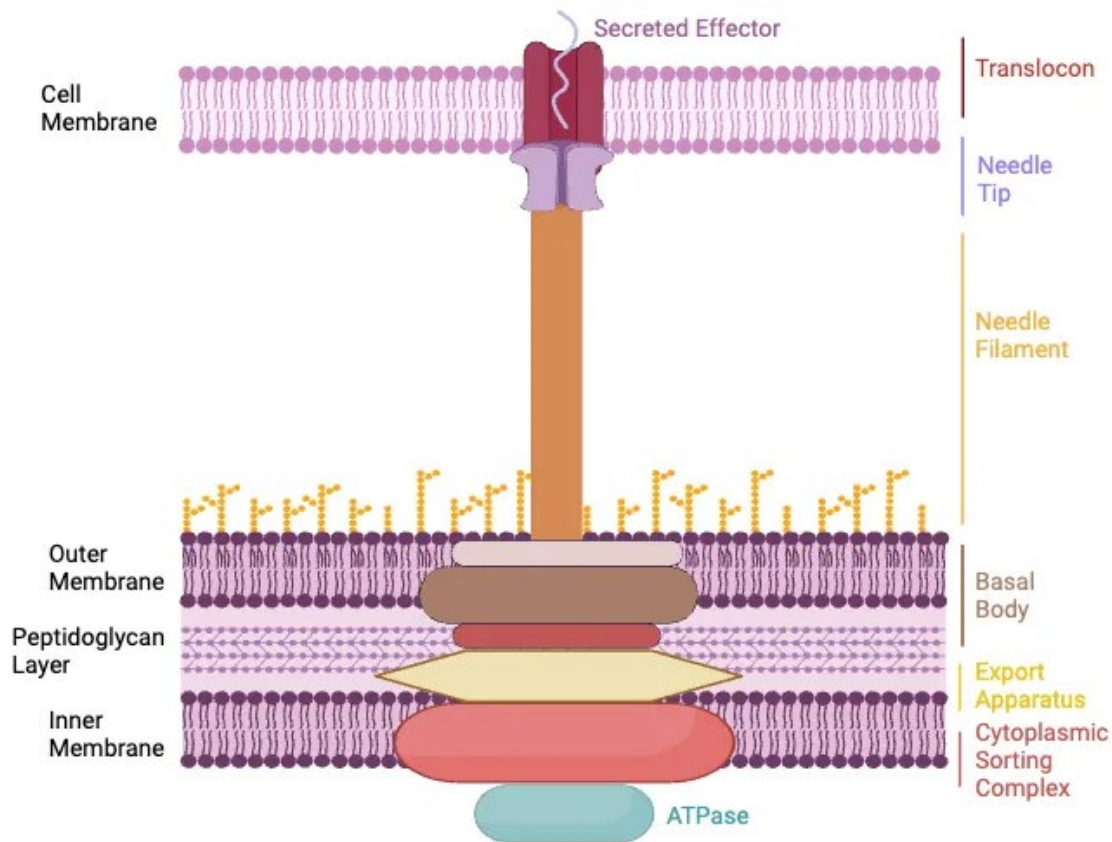


**Figure 1.** T3SS general structure with color-coded and labeled sections

In *Salmonella*, the Salmonella Pathogenicity (SPI-1) virulence factor codes for the T3SS that enables bacterial invasion into host cells, where SPI-1 delivered effectors restructure the cytoskeleton of the host cell to force phagocytosis of the *Salmonella* pathogen<sup>12, 13</sup>. This process is critically dependent on the hexameric ATPase in the cytoplasmic complex, which is known as InvC in *Salmonella*. InvC is composed primarily of

three folded domains: the N-terminal involved in the oligomerization of InvC<sup>14</sup>; the conserved ATPase catalytic domain; and the C-terminal, which is potentially involved in recognizing chaperone-effector complexes<sup>15</sup>. InvC plays a role in recognizing and binding the chaperone-effector complex, catalyzing ATP-fueled effector removal, and unfolding effectors in preparation for secretion<sup>15</sup>. It is vital for *Salmonella* proliferation, for strains with loss-of-function mutant InvC were unable to successfully invade intestinal epithelial cells after the catalytic phosphate-binding loop motif (P-loop) was modified<sup>14</sup>.

The necessity of InvC for virulence and its conserved structure across several pathogen species makes it an attractive target for T3SS inhibition. InvC is also highly related to several other T3SS ATPases, like *Shigella* Spa47, *Yersinia* YscN, *E. coli* EscN, and *Pseudomonas* HrcN, sharing 38-75% of its sequence with these orthologs<sup>16</sup>—giving it potential as a target for broad-spectrum activity. The dysfunctionality of ATPase-knock-out mutants is not restricted to *Salmonella*; in *E. coli*, deletion of the EscN gene (an ortholog to InvC) renders the pathogen unable to develop or secrete virulence factors<sup>17</sup>. Similarly, in *Y. enterocolitica*, deletion of the YscN gene (another ortholog to InvC) abolishes the secretion of bacterial effectors<sup>18</sup>. In *Salmonella*, when InvC is heavily destabilized, mutant strains are defective for translocation of effectors, bacterial egress, cytosolic colonization, and vacuolar replication<sup>19</sup>. In addition, inhibition of T3SS ATPase avoids the risk of cross-reaction between T3SS ATPase inhibitors and human ATPase enzymes because bacterial ATPase and human ATPase share less than 25% of their sequences and their active sites are structurally different<sup>5</sup>. Though there are many existing inhibitors of *Salmonella* T3SS, none have been shown to target the InvC protein vital for combating antibacterial resistance<sup>20, 21, 22, 23, 24</sup>.

In this work, we identify potential inhibitors of the *Salmonella* ATPase InvC protein using in-silico molecular docking and structure-based virtual screening—a promising tool for drug discovery enabled by newly available protein crystallography structures<sup>25</sup> and ligand libraries<sup>26</sup>. Computationally predicting the binding conformations of ligands to a receptor allows for the rapid screening of thousands of potential ligands to find the most viable lead compounds, an efficient precursor to traditional synthesis and biological assays<sup>27</sup>. The compounds with the most negative binding energies (in kcal/mol) represent the most stable conformations; the lower the binding energy, the better a ligand can bind to the active site and is therefore predicted to be a more potent inhibitor. Here, we use these binding scores to identify lead compounds with the most potential. Additionally, catalogs of commercially available drug structures enable the targeted screening of compounds with known properties and metabolic activity. Especially with the availability of the Zinc database<sup>28</sup>, we were able to preliminarily filter out small molecules with nonoptimal drug-likeness (an estimation of a compound's in-vivo potential based on its physiochemical properties) by selecting ligands with favorable molecular weight and lipophilicity—factors that have been demonstrated to impact molecular absorption, metabolism, and other factors (more details in methods/results)<sup>29</sup>.

In this study, we screened thousands of potential ligands from the Zinc database and utilized AutoGrow4, an open-source structure-based drug design tool, to evolve potent inhibitors into novel drug-like compounds with optimized properties<sup>30</sup>. We present over a dozen lead compounds derived from ten generations of ligand evolution with the highest binding affinities, as well as an evaluation of an entirely open-source route to novel inhibitor identification through the examination of the software's efficacy across generations.

## Results

We computationally screened selected molecules from the Zinc database against the active site of the InvC protein through AutoGrow4 for a total of 10 generations against the *bsdX* model of InvC from the Protein Data Bank<sup>31</sup>. Out of the *Salmonella* InvC models in the Protein Data Bank, we chose *bsdX* because it contains ATP-gamma-s, the ligand used for investigation in the reference literature<sup>32</sup>. For the binding site, we targeted the P-loop (amino acid residues 162-166) located in the ATPase catalytic core<sup>32</sup>, as well as surrounding residues shown to interact with ligands in the binding site. When ATP-gamma S is bound to the enzyme, the phosphate

groups form hydrogen bonds with G164 and T166, and a salt bridge with K165; the adenine group is stabilized by a pi-stacking bond with Y338 and forms a hydrogen bond with V411. As shown, this loop is highly relevant for ATP recognition and synthesis.

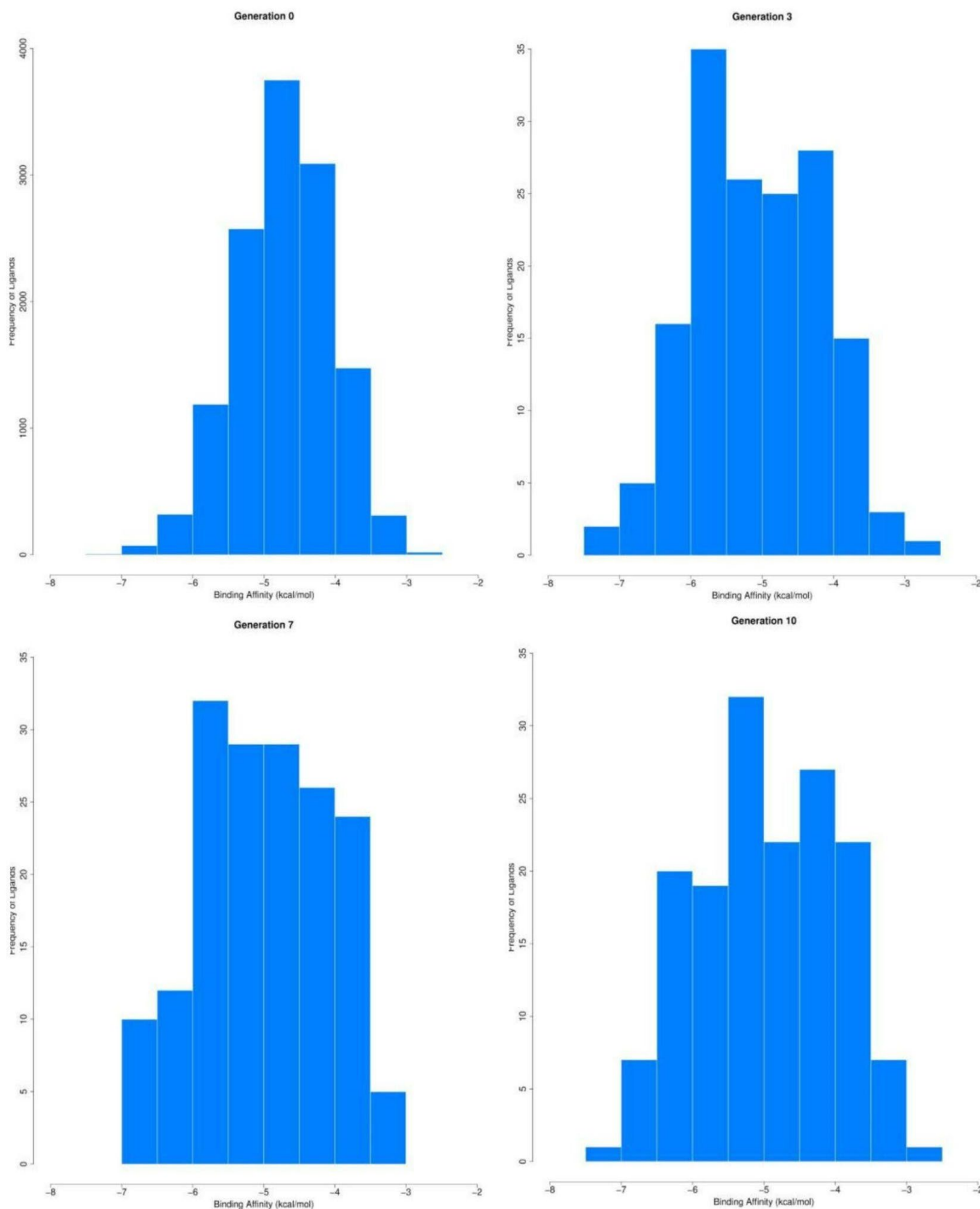
Since AutoGrow tends to create population homogeneity, convergence, and undesirable moieties after longer runs<sup>30</sup>, we executed AutoGrow for 10 generations until improvement began to stall. We noticed compound fitness improving quickly in the first few generations and progress slowing in later generations, so compound suitability was unlikely to improve upon further experimentation. One limitation of this study is the slight drop-off in ligand fitness in the latter half of the generations, which reduced the versatility of our screened ligands. Additionally, we found that AutoGrow works best with well-researched proteins such as PARP-1<sup>30</sup>, so the relative novelty of *6sdx* may also inhibit experimental efficacy.

Shown below in Figure 2 is the binding pocket we used on 6SDX, including the main P-loop (G162 - M167) and other amino acids that ATP has been shown to interact with while binding. Using these amino acids, we determined the size of the binding pocket shown in red. Also shown is the structure of the amino acids in the binding site and their polar interactions with surrounding residues. The critical interactions between the binding site and the ligand in this pocket combined with the pocket's remodeling upon binding imply that inhibitors here would significantly impact InvC function<sup>31</sup>.



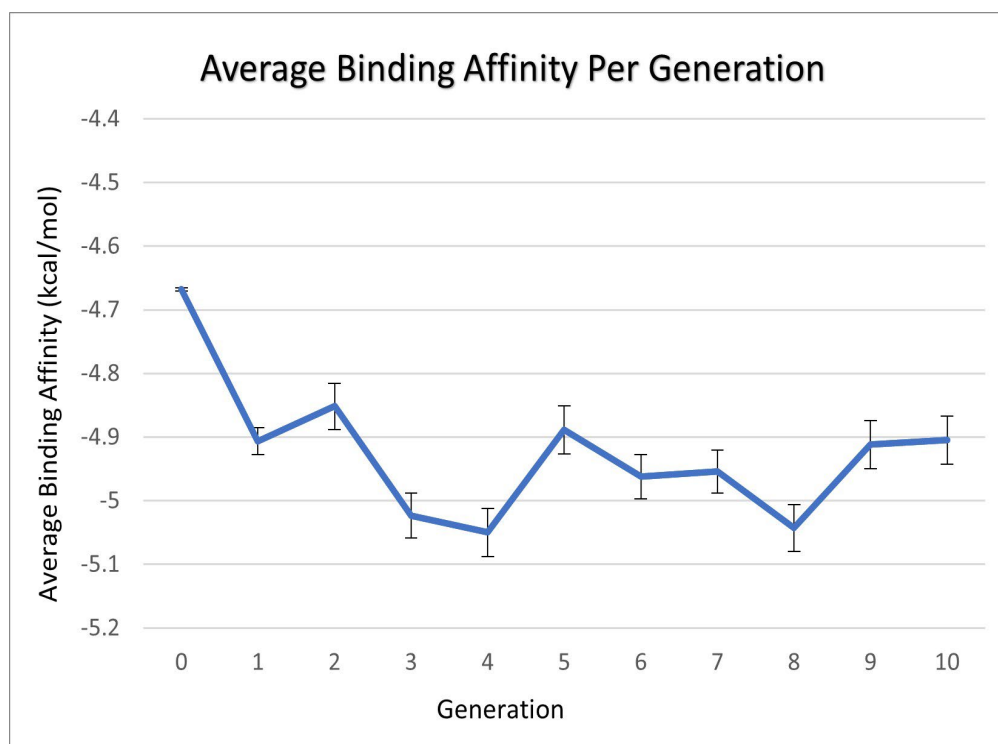
**Figure 2.** Binding pocket on 6SDX 3-D structure

Figure 3a depicts the evolution of the ligands from generation 0, generation 3, generation 7, and generation 10. Generation 0 depicts the spread of binding affinities of ligands from the Zinc database, while generations 3, 7, and 10 depict data from novel ligands developed by Autogrow through mutations and crossovers. Between generation 0 and generation 10, there is a visible increase in the proportion of ligands with binding affinities between -5 to -7.



**Figure 3a.** Autodock Vina Binding affinities from generations 0, 3, 7, and 10

A shift from generation 0 to generation 3 is also present, though less obvious. Proportionally, there is a higher number of ligands with binding affinities from -4.5 to -6.5 in generation 3 compared to generation 0. The peak in the generation 3 graph occurs at -5.5 to -6.0 kcal/mol, while the peak in the generation 0 graph occurs at -4.5 to -5.0 kcal/mol. From generation 3 to generation 7, the spread of the graph decreases, and the graph shows an increased proportion of compounds with binding affinities from -6.0 to -7.0. The peak of the graph remains at the same binding affinity. From generation 7 to generation 10, the proportion of compounds with binding affinities better than -5.0kcal/mol appears to decrease slightly, indicative of the previously discussed stagnation in later generations.



**Figure 3b.** Average binding affinity across generations

In evaluating AutoGrow, we conducted 2-sample T-tests comparing the mean binding affinity of each generation to the mean binding affinity of generation 0. Since each generation represents a small sample of an infinite population of compounds, we can use a t-test to estimate the true mean binding affinity of ligands in each generation and test for significant improvement across generations. All three conditions required for a T-test are met by each sample: the samples are random, chosen independently, and display relatively normal distributions.

The mean binding affinity of each generation was compared to the mean binding affinity of generation 0. We hypothesized that the mean binding affinity of generations 1-10 would be significantly smaller than the mean binding affinity of generation 0, setting a standard alpha-value of 0.05. The results of the significance test are shown below.

**Table 1.** Mean binding affinity score of each generation vs. generation 0

Generation	Sample Size	Mean Binding Affinity (kcal/mol)	Std. Dev (kcal/mol)	P-value
0	12787	-4.665	0.661	N/A
1	478	-4.906	0.928	$1.505 * 10^{-8}$
2	153	-4.852	0.904	0.0171
3	156	-5.023	0.879	$5.56 * 10^{-8}$
4	152	-5.050	0.942	$6.98 * 10^{-7}$
5	148	-4.889	0.919	0.00185
6	152	-4.9625	0.859	$1.803 * 10^{-5}$
7	167	-4.954	0.879	$1.834 * 10^{-5}$
8	163	-5.044	0.950	$5.455 * 10^{-7}$
9	165	-4.912	0.976	$7.19 * 10^{-4}$
10	158	-4.905	0.962	0.001

Every generation expresses significantly better binding affinities than generation 0, as all p-values shown are less than 0.05. In comparison to the original compounds of the ZINC database, Autogrow's algorithms were able to generate novel small-molecule inhibitors that are significantly better. However, this table does not reflect significant improvement over successive generations; the small p-values could reflect an improvement in mean binding affinity in one generation but relative stagnation over the rest.

In order to study AutoGrow's efficiency over each generation, we also did 2-sample t-tests between each generation and the generation prior. We hypothesized a significant improvement in mean binding affinity from generation  $n$  to generation  $n + 1$ , with a standard alpha-value set to 0.05. Results are shown in the table below.

**Table 2.** Mean binding affinity score of each generation vs. the previous generation

Generation	P-value
0 & 1	$1.49 * 10^{-8}$
1 & 2	0.74
2 & 3	0.046
3 & 4	0.602
4 & 5	0.934
5 & 6	0.236
6 & 7	0.533
7 & 8	0.189
8 & 9	0.891
9 & 10	0.526
0 & 1	$1.49 * 10^{-8}$

Looking at this table, only two p-values are below the critical value ( $<0.05$ ): there is significant improvement in mean binding affinity from generation 0 to generation 1, and from generation 2 to generation 3. Although there is overall progress after generation 1 (see Table 1), AutoGrow seems to stagnate without consistent improvement between generations, with the exception of generation 3. This may be due to the relatively

unexplored structure of *6sdx* compared to other proteins, especially the PARP-1 receptor that AutoGrow 4 was tested on. Without enough information on protein structure, AutoDock Vina may not be able to accurately predict interactions during ligand binding.

Finally, we present the lead compounds identified among 14690 evaluated ligands. Across generations, our adaptive screening produced 14 compounds with binding affinities at or above  $-7.0$  kcal/mol, five of which are original Zinc Database compounds, and the others novel mutations produced by AutoGrow4. The structure, highest binding affinity, and the first six digits of the compound code are provided in Figure 4.

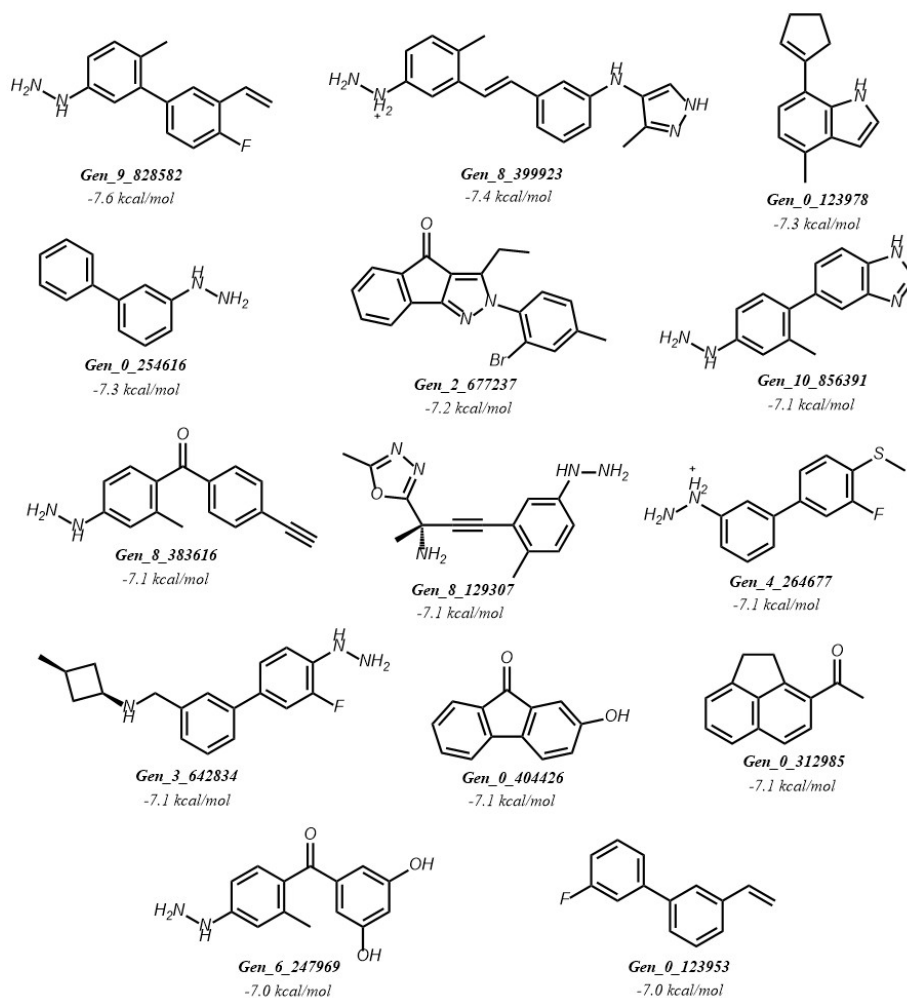


**Figure 4.** Best-performing compounds across all generations by binding affinity

## Discussion

While these compounds must be evaluated *in vitro* to reach definite conclusions, our novel ligands exhibit promising binding properties against *Salmonella* ATPase. Because heavy displacement of the P-loop is associated with ATP-analog binding, the disruption of those critical domains is likely to halt ATP hydrolysis<sup>32</sup>. Without a functional ATPase enzyme, almost all pathogens are unable to properly inject effectors. This sabotages their ability to subvert host cell function, alter cytoskeleton structure, and evade immune system responses<sup>6</sup>. Although the exact mechanisms linking ATP hydrolysis to the formation of the injectosome and secretion of



protein effectors are not fully understood, several experiments have found a direct causal relationship between loss-of-function InvC mutations and loss of virulence<sup>33, 34</sup>.

In addition, the small molecules exhibit optimal molecular size and lipophilicity conditions that maximize clinical potential, making them promising agents against antibiotic-resistant *Salmonella*. Because many T3SS-dependent bacteria have similar secretion systems, the compounds identified here for *Salmonella* ATPase inhibition are favorable for broad-spectrum therapeutic development. The central T3SS ATPase among gram-negative bacteria is highly conserved, generating potential for T3SS inhibitors to treat a variety of infections.

The work presented also evaluates AutoGrow4's efficacy as a novel drug-design tool, for it is one of few open-source ligand evolution programs. AutoGrow4 enables discovery at a speed much faster than *ex silico* experimentation, with the capability to screen thousands of compounds and evolve them into a smaller group of energetically favorable ligands, introducing many possibilities for drug discovery and lead optimization. Although AutoGrow4 works less optimally without extensive knowledge of the target binding pocket and known inhibitors, there is still clear improvement in mean binding affinity across ten generations in our experiment. In addition, most compounds generated by AutoGrow are chemically feasible, and several filters (such as the Lipinski Strict Filter, the Ghose filter, or the VandeWaterbeemd Filter) can customize compound results<sup>30</sup>.

In combination with open-source chemical databases like ZINC, our work presents a viable and entirely open-source workflow for the discovery of chemical inhibitors and lead optimization toward the treatment of new biological targets. We demonstrate the plausibility of this workflow by presenting fourteen promising compounds for T3SS inhibition that surpass the binding efficacy of many FDA-approved therapeutics<sup>40</sup>. In an era of widespread antibiotic resistance and skyrocketing demand for improved therapeutics, exploring new pathways for efficient drug discovery is vital.

## Limitations

Our study is limited by computational capabilities, available research on the ATPase InvC protein, and laboratory access. Thus, directions for future research include expanding the scope of generation 0 ligands and synthesizing the best-performing lead compounds for subsequent in-vitro evaluation. It is impossible to confirm a compound's inhibitory ability in pathogens only by knowing its computational binding efficacy. However, with protein structure modeling algorithms growing fast using Deep Learning and AI, AutoGrow4 should soon have even broader applications and provide more accurate results<sup>30</sup>.

## Methods

### Receptor Preparation

The *6sdx* protein was obtained as a .pdb file from RCSB<sup>31</sup>. The protein was prepared for docking in PyMol, with all ligands removed (labeled residues 501-506 in the protein sequence). All water was removed. The protein was properly protonated using the PDB2PQR webserver tool from UCSF<sup>36</sup>, and the resulting .pqr file was converted back to .pdb using Open Babel<sup>37</sup>.

In order to obtain the center of the binding pocket and the size of the binding pocket, the open-source Python algorithm Scoria was used<sup>38</sup>. Amino acid residues 162-167, 338, and 409- 411 were used as the binding pocket, justified in the results section. This gave us a binding pocket center of (34.681, -13.6825, 10.3986) for x, y, and z respectively, and a binding pocket size with dimensions (12.0, 20.0, 12.0), for length, width, and height.

### Ligand Sourcing

The initial pool of compounds is sourced from the ZINC-15 database, which has over 120,000,000 commercially available compounds for virtual screening. Selected compounds had a molecular weight between 150 to 250Da and a LogP value less than 5, with any level of reactivity. Compounds were then filtered with the Lipinski strict filter and converted into SMILE strings. The compounds were sorted into functional groups, and 100 compounds were randomly selected from each functional group. In total, this created an initial pool of 16,603 compounds (though generation 0 is slightly smaller due to AutoGrow's inability to dock certain compounds in time).

## AutoGrow4

To produce novel compounds with improved binding affinities, we used AutoGrow4<sup>30</sup>. AutoGrow can draw from an initial pool of molecules to synthesize new generations of ligands, and ranks this new generation by docking each compound, taking the top molecules, or seeds, of each generation for the next. AutoGrow generates this new population through three different methods: an elitism operator, a mutation operator, and a crossover operator, which ideally creates a pool of compounds with better binding affinity than the previous. The *6sdx* protein was processed and submitted as a .pdb, and the binding coordinates were obtained using Scoria, as explained previously. We ran AutoGrow for 10 generations, using MGLTools for conversion from .pdb to .pdbqt, and the default RDKit cheminformatics reactions as the reaction library. AutoGrow 4 uses QuickVina 2 as its default docking platform<sup>39</sup>, which we did not modify. For molecular filters, we used the Lipinski Leniency Filter, as well as the Rank Selector for subsequent generations to prevent duplicates. In the first generation, we seeded 70 molecules from mutations and crossovers to the next generation alongside 100 elite molecules; for each subsequent generation, we seeded 50 molecules from mutations and crossovers, alongside 100 elite molecules for the next generation. The molecules from the Zinc database were first docked and scored to create a generation 0 before the selection process began for generation 1. This gave us a compiled folder of the molecules created each generation, their binding affinity, and the SMILE string for the molecule. The data was then compiled into graphs and tables for processing.

## Acknowledgments

We would like to thank Ilinca Flacau for her programming support in sorting and compiling data for our analysis and figures. We would also like to acknowledge BioRender.com for its use in figure design.

## References

1. World Health Organization. Antibiotic Resistance. <https://www.who.int/news-room/fact-sheets/detail/antibiotic-resistance> (2020).
2. World Health Organization. "Report signals increasing resistance to antibiotics in bacterial infections in humans and need for better data." <https://www.who.int/news/item/09-12-2022-report-signals-increasing-resistance-to-antibiotics-in-bacterial-infections-in-humans-and-need-for-better-data> (2022).
3. D. V. T. Nair., K Venkitanarayanan, A Kollanoor Johny. Antibiotic-resistant salmonella in the food supply and the potential role of antibiotic alternatives for control. *Foods*, 7, 167. <https://doi.org/10.3390/foods7100167> (2018).
4. Center for Disease Control. The biggest antibiotic-resistant threats in the U.S. <https://www.cdc.gov/drugresistance/biggest-threats.html#sal> (2019).

5. MC Duncan, RG Linington, V Auerbuch. Chemical inhibitors of the type three secretion system: disarming bacterial pathogens. *Antimicrobials Agents for Chemotherapy*, 56, 5433-41. doi: 10.1128/AAC.00975-12 (2012).
6. HB Case, DS Mattock, BR Miller, NE Dickenson. Novel noncompetitive type three secretion system ATPase inhibitors shut down Shigella effector secretion. *Biochemistry*, 59, 2667–2678. <https://doi.org/10.1021/acs.biochem.0c00431> (2020).
7. Supratim Dey, Amritangshu Chakravarty, Pallavi Guha Biswas, Roberto N. De Guzman. The type III secretion system needle, tip, and translocon. *Protein Science*, 28, 1582-1593. Doi: 10.1002/pro.3682 (2019).
8. W Samuel, G Iwan, M Silke, S Nidhi, ETV Claudia, W Sibel. Bacterial type III secretion systems: a complex device for the delivery of bacterial effector proteins into eukaryotic host cells, *FEMS Microbiology Letters*, 365, 201. Doi: 10.1093/femsle/fny201 (2018).
9. Y Wang, M Hou, Z Kan, G Zhang, Y Li, L Zhou, and C Wang. Identification of Novel Type Three Secretion System (T3SS) Inhibitors by Computational Methods and Anti-Salmonella Evaluations. *Frontiers in Pharmacology*, 12, 764191. doi: 10.3389/fphar.2021.764191 (2021).
10. B Coburn, I Sekirov, BB Finlay. Type III secretion systems and disease. *Clinical Microbiol Review*, 20, 535-549. doi:10.1128/CMR.00013-07 (2007).
11. JA Hotinger, HA Pendergrass, AE May. Molecular Targets and Strategies for Inhibition of the Bacterial Type III Secretion System (T3SS); Inhibitors Directly Binding to T3SS Components. *Biomolecules*, 2021, 316. doi:10.3390/biom11020316 (2021).
12. L Lou, P Zhang, R Piao and Y Wang. Salmonella Pathogenicity Island 1 (SPI-1) and Its Complex Regulatory Network. *Frontiers in Cellular and Infection Microbiology*, 9, 270. doi: 10.3389/fcimb.2019.00270 (2019).
13. PJ Hume, V Singh, AC Davidson, V Koronakis. Swiss Army Pathogen: The Salmonella Entry Toolkit. *Frontiers in Cellular and Infection Microbiology*, 7, 348. doi:10.3389/fcimb.2017.00348 (2017).
14. Y Akeda, J Galán. Genetic Analysis of the Salmonella enterica Type III Secretion-Associated ATPase InvC Defines Discrete Functional Domains. *ASM Journal of Bacteriology*, 186, 2402 - 2412. <https://doi.org/10.1128/jb.186.8.2402-2412.2004> (2004).
15. Y Akeda, J Galán. Chaperone release and unfolding of substrates in type III secretion. *Nature*, 437, 911–915. <https://doi.org/10.1038/nature03992> (2005).
16. R Zarivach, M Vuckovic, W Deng, BB Finlay, & NCJ Strynadka. Structural analysis of a prototypical ATPase from the type III secretion system. *Nature Structural & Molecular Biology*, 14, 131–137. doi:10.1038/nsmb1196 (2007).
17. W. Swietnicki, D. Carmany, M. Retford, M. Guelta, R. Dorsey, J. Bozue, MS Lee, MA Olson. Identification of Small-Molecule Inhibitors of Yersinia pestis Type III Secretion System YscN ATPase. *PLoS One*, 6, e19716. doi:10.1371/journal.pone.0019716 (2011).
18. S. Woestyn, A. Allaoui, P. Wattiau, G.R. Cornelis. YscN, the putative energizer of the Yersinia Yop secretion machinery. *ASM Journal of Bacteriology*, 176, 1561-1569. Doi: 10.1128/jb.176.6.1561-1569.1994 (1994).
19. J. A. Klein, J. R. Grenz, J. M. Slauch, L. A. Knodler. Controlled Activity of the Salmonella Invasion-Associated Injectisome Reveals Its Intracellular Role in the Cytosolic Population. *ASM mBio*, 8. doi: 10.1128/mbio.01931-17 (2017).
20. DL Hudson, AN Layton, TR Field, AJ Bowen, H Wolf-Watz, M Elofsson, MP Stevens, EE Galyov. Inhibition of type III secretion in Salmonella enterica serovar Typhimurium by small-molecule inhibitors. *Antimicrobial Agents and Chemotherapy*, 51, 2631-5. doi: 10.1128/AAC.01492-06 (2007).

21. LN Nesterenko, NA Zigangirova, ES Zayakin, SI Luyksaar, NV Kobets, DV Balunets, LA Shabalina, TN Bolshakova, OY Dobrynina, AL Gintsburg. A small-molecule compound belonging to a class of 2,4-disubstituted 1,3,4-thiadiazine-5-ones suppresses Salmonella infection in vivo. *The Journal of Antibiotics*, 69, 422-7. doi: 10.1038/ja.2015.131 (2016).
22. HB Felise, HV Nguyen, RA Pfuetzner, KC Barry, SR Jackson, MP Blanc, PA Bronstein, T Kline, SI Miller. An inhibitor of gram-negative bacterial virulence protein secretion. *Cell Host Microbe*, 4, 325-36. doi: 10.1016/j.chom.2008.08.001 (2008).
23. Y Wang, M Hou, Z Kan, G Zhang, Y Li, L Zhou, C Wang. Identification of Novel Type Three Secretion System (T3SS) Inhibitors by Computational Methods and Anti-Salmonella Evaluations. *Frontiers in Pharmacology*, 12, 764191. doi: 10.3389/fphar.2021.764191 (2021).
24. R Boonyom, S Roytrakul, P Thinwang. A small molecule, C<sub>24</sub>H<sub>17</sub>CIN<sub>4</sub>O<sub>2</sub>S, inhibits the function of the type III secretion system in Salmonella Typhimurium. *Journal of Genetic Engineering and Biotechnology*, 20, 54. doi: 10.1186/s43141-022-00336-1 (2022).
25. H.M. Berman, J. Westbrook, Z. Feng, G. Gilliland, T.N. Bhat, H. Weissig, I.N. Shindyalov, P.E. Bourne. The Protein Data Bank. *Nucleic Acids Research*, 28, 235-242 <https://doi.org/10.1093/nar/28.1.235> (2000).
26. EHB Maia, LC Assis, TA Oliveira, AM Silva, AG Taranto. Structure-Based Virtual Screening: From Classical to Artificial Intelligence. *Frontiers in Chemistry*, 8,343. doi: 10.3389/fchem.2020.00343 (2020).
27. XY Meng, HX Zhang, M Mezei, M Cui. Molecular docking: a powerful approach for structure-based drug discovery. *Current Computer Aided Drug Design*, 7,146-57. doi: 10.2174/157340911795677602 (2011).
28. JJ Irwin, KG Tang, J Young, C Dandarchuluun, BR Wong, M Khurelbaatar, YS Moroz, J Mayfield, RA Sayle. ZINC20—A Free Ultralarge-Scale Chemical Database for Ligand Discovery. *Journal of Chemical Information and Modeling*, 60, 6065-6073. DOI: 10.1021/acs.jcim.0c00675 (2020).
29. ZY Yang, JH He, AP Lu, TJ Hou, DS Cao. Application of Negative Design To Design a More Desirable Virtual Screening Library. *Journal of Medicinal Chemistry*, 63, 4411-4429. DOI: 10.1021/acs.jmedchem.9b01476 (2020).
30. JO Spiegel, JD Durrant. AutoGrow4: an open-source genetic algorithm for de novo drug design and lead optimization. *Journal of Cheminformatics*, 12, 25. Doi: 10.1186/s13321-020-00429-4 (2020).
31. I Bernal, J Roemermann, L Flacht, M Lunelli, C Utrecht, M Kolbe. Salmonella ATPase InvC with ATP gamma S. doi.org/10.2210/pdb6SDX/pdb (2019).
32. I Bernal, J Roemermann, L Flacht, M Lunelli, C Utrecht, M Kolbe. Salmonella ATPase InvC with ATP gamma S. *Protein Science*, 28, 1888-1901. doi.org/10.2210/pdb6SDX/pdb (2019).
33. K Eichelberg, CC Ginocchio, JE Galán JE. Molecular and functional characterization of the *Salmonella typhimurium* invasion genes invB and invC: homology of InvC to the F<sub>0</sub>F<sub>1</sub> ATPase family of proteins. *Journal of Bacteriology*, 176, 4501-10. doi: 10.1128/jb.176.15.4501-4510.1994 (1994).
34. JM Ritchie, MK Waldor. The locus of enterocyte effacement-encoded effector proteins all promote enterohemorrhagic Escherichia coli pathogenicity in infant rabbits. *ASM Infection and Immunity*, 73,1466-74. doi: 10.1128/IAI.73.3.1466-1474.2005 (2005).
35. JL Burgess, RA Burgess, Y Morales, JM Bouvang, SJ Johnson, NE Dickenson. Structural and Biochemical Characterization of Spa47 Provides Mechanistic Insight into Type III Secretion System ATPase Activation and Shigella Virulence Regulation. *Journal of Biological Chemistry*, 291, 25837-25852. Doi: 10.1074/jbc.M116.755256 2016 (2016).
36. E Jurrus, D Engel, K Star, K Monson, J Brandi, LE Felberg, DH Brookes, L Wilson, J Chen, K Liles, M Chun, P Li, DW Gohara, T Dolinsky, R Konecny, DR Koes, JE Nielsen, T Head-Gordon,

- W Geng, R Krasny, GW Wei, MJ Holst, JA McCammon, NA Baker. Improvements to the APBS biomolecular solvation software suite. *Protein Science*, 27, 112-128. doi: 10.1002/pro.3280 (2017).
37. NM O'Boyle, M Banck, CA James, C Morley, T Vandermeersch, GR Hutchison. Open Babel: An open chemical toolbox. *Journal of Cheminformatics*, 3, 33. DOI:10.1186/1758-2946-3-33 (2011). Version 2.2.0, Accessed 08/2023.
38. P Ropp, A Friedman, JD Durrant. Scoria: a Python module for manipulating 3D molecular data. *Journal of Cheminformatics*, 9, 52. doi: 10.1186/s13321-017-0237-8 (2017).
39. A Alhossary, SD Handoko, Y Mu, CK Kwok. Fast, Accurate, and Reliable Molecular Docking with QuickVina 2. *Bioinformatics*, 31, 2214–2216. doi: 10.1093/bioinformatics/btv082 (2015).
40. AK Ray, PS Sen Gupta, SK Panda, S Biswal, U Bhattacharya, MK Rana. Repurposing of FDA-approved drugs as potential inhibitors of the SARS-CoV-2 main protease: Molecular insights into improved therapeutic discovery. *Computers in Biology and Medicine*, 142,105183. doi: 10.1016/j.combiomed.2021.105183 (2022).